Published in final edited form as:
Mech Ageing Dev. 2020 September 01; 190: 111322. doi:10.1016/j.mad.2020.111322.

A new model to investigate UVB-induced cellular senescence and pigmentation in melanocytes

Ines Martic[a,b], **Sophia Wedel**[a,b], **Pidder Jansen-Dürr**[a,b], **Maria Cavinato**[a,b,*]

[a]Institute for Biomedical Aging Research, Universität Innsbruck, Austria

[b]Center for Molecular Biosciences Innsbruck (CMBI), Innsbruck, Austria

Abstract

Ultraviolet (UV) light is known to potentially damage human skin and accelerate the skin aging process. Upon UVB exposure, melanocytes execute skin protection by increasing melanin production. Senescent cells, including senescent melanocytes, are known to accumulate in aged skin and contribute to the age-associated decline of tissue function. However, melanocyte senescence is still insufficiently explored. Here we describe a new model to investigate mechanisms of UVB-induced senescence in melanocytes and its role in photoaging. Exposure to mild and repeated doses of UVB directly influenced melanocyte proliferation, morphology and ploidy. We confirmed UVB-induced senescence with increased senescence-associated β-galactosidase positivity and changed expression of several senescence markers, including p21, p53 and Lamin B1. UVB irradiation impaired proteasome and increased autophagic activity in melanocytes, while expanding intracellular melanin content. In addition, using a co-culture system, we could confirm that senescence-associated secretory phenotype components secreted by senescent fibroblasts modulated melanogenesis. In conclusion, our new model serves as an important tool to explore UVB-induced melanocyte senescence and its involvement in photoaging and skin pigmentation.

Keywords

Senescence; Skin aging; Melanogenesis; Pigmentation; Proteostasis

1 Introduction

The skin is the largest organ of the human body and performs several functions, including protection against damage caused by environmental factors (Prieux et al., 2020). Skin aging is caused by two distinct, but overlapping, mechanisms – intrinsic and extrinsic aging. Intrinsic aging affects not only the skin, but all tissues and organs of the body and is understood as time-depending and influenced by genetic background (Abd El-Aal et al.,

*Corresponding author at: Institute for Biomedical Aging Research, Universität Innsbruck, Rennweg 10, 6020, Innsbruck, Austria. maria.cavinato-nascimento@uibk.ac.at (M. Cavinato).

Declaration of Competing Interest
The authors declare that there are no competing interests associated with this manuscript.

Europe PMC Funders Author Manuscripts

2012; Cavinato et al., 2017). In addition, skin is continuously exposed to environmental factors, which contribute to the process of extrinsic skin aging. Among the factors that cause damage to the skin, UV radiation is considered the most harmful (Cavinato, 2020; Krutmann et al., 2017). UVB rays are known to directly damage DNA, to promote the accumulation of reactive oxygen species (ROS) and subsequent oxidation of proteins and lipids (Greussing et al., 2013).

Cellular senescence is a state of proliferative arrest characterized by significant changes in the morphology and functionality of cellular components (López-Otín et al., 2013). Accumulation of senescent cells in different tissues contributes to the decline of functions characteristic of the aging process (Baker et al., 2016; Tominaga, 2015). Specifically in the skin, senescent fibroblasts contribute to aging by secretion of extracellular matrix degrading matrix metalloproteases (MMPs) and other senescence-associated secretory phenotype (SASP) components (Toutfaire et al., 2017; Waldera Lupa et al., 2015; Wang and Dreesen, 2018). Senescence of melanocytes has been insufficiently explored but recent studies have reported that senescent melanocytes accumulate in human skin where they contribute to the aging process by impairing proliferation of the neighboring keratinocytes (Victorelli et al., 2019; Waaijer et al., 2016).

A decisive characteristic of skin aging is the accumulation of oxidized and damaged proteins, which leads to an impaired cellular protein homeostasis (Cavinato and Jansen-Dürr, 2017). In a previous publication, we have demonstrated that damaged proteasome activity is compensated by increased autophagy in a model of UVB-induced senescence of fibroblasts and that these events are essential for the establishment of the senescence phenotype (Cavinato et al., 2016). Skin aging-associated proteostatic changes also occur in keratinocytes (Eckhart et al., 2019). Autophagy is closely connected to the regulation of synthesis and removal of melanosomes and defects in either one of these mechanisms potentially causes pigmentary disorders (Ho and Ganesan, 2011; Wang et al., 2019b). The exact role of proteasome and autophagic activity in melanocytes - especially after UV-exposure of the cells - is not yet understood.

Age spots typically occur in chronically sun-exposed skin and the appearance of this aberrant pigmentation has been associated with irregularities in melanocyte distribution, enhanced melanogenic signalling and decreased melanosome removal (Barysch et al., 2019; Choi et al., 2017; Haddad et al., 1998). Recently, it has been demonstrated that the occurrence of age spots is not solely influenced by changes in melanocytes, but by the deregulated secretion of molecules produced by photoaged keratinocytes and fibroblasts emphasizing the complexity of underlying factors driving photoaging and the development of senile lentigines (Bellei and Picardo, 2020). However, there is still a big gap in our understanding of the underlying mechanisms by which senescent cells contribute to the photoaging of the skin. Thus, the establishment of models that reflect these processes is increasingly necessary.

Here, we introduce a new model to study melanocyte senescence during the process of photoaging. Using this model, we investigated the direct influence of UVB irradiation on melanocyte proteasome and autophagic activity in cell monolayers. In addition, we

examined the potential of a previously established UVB-induced senescence model of dermal fibroblasts (Cavinato et al., 2016; Greussing et al., 2013) to influence aspects of melanocyte's biology in a co-culture system.

2 Material and methods

2.1 Chemicals

All chemicals were purchased from Sigma (Steinheim, Germany) unless stated otherwise.

2.2 Cell Culture and UVB irradiation

Human dermal fibroblasts (HDFs) derived from neonatal foreskin (ATCC, Manassas, USA #SCRC-1042), HEK293-T cells and U2OS cells were cultivated with normal DMEM supplemented with 10 % FCS, 2 % glutamine and 1 % penicillin/streptomycin. Primary human skin epidermal melanocytes (HSEM) (CellSystems Biotechnologie Vertrieb, Germany) were cultivated in DermaLife basal medium supplemented with DermaLife M Life Factors (CellSystems Biotechnologie Vertrieb, Germany). UVB irradiation of HDFs was performed twice a day for four days with 0.05 J/cm^2 per treatment as described (Greussing et al., 2013). After the fourth day of treatment (UVB D4), cells were allowed to recover and were used for further experiments. Treatment of melanocytes with UVB was performed in a similar way using a dose of 0.125 J/cm^2. Cell number was determined using CASY Cell Counter (Schärfe System, Germany). Relative cell numbers were calculated by normalizing the number of control cells to 100 %. Cumulative population doublings (cPDLs) were calculated as described (Hutter et al., 2004). Changes in cell morphology and size were monitored by light microscopy using Nikon eclipse TE300 inverted microscope (Nikon, The Netherlands). Analysis of cell surface area was performed in ImageJ software.

2.3 Lentiviral transduction for stable overexpression

Degron-destabilized green fluorescent protein (GFP-degron) expressing melanocytes were produced by lentiviral infection as described (Greussing et al., 2012).

2.4 Co-Culture

For co-culture experiments, UVB-irradiated HDFs (UVB D7) and the corresponding controls (Ctrl D7) were seeded on the insert of transwell co-culture plates (Corning™ Costar™ Transwell™ permeable supports from Corning incorporated, USA). HSEM were seeded at the bottom of a 6-well plate. One day later, inserts containing HDFs were moved to the 6-well-plates containing melanocytes to establish the co-culture system. Co-culture was kept in melanocyte culture medium for the following three days as described (Yoon et al., 2018). At the end of the third day, cells were processed for further experiments.

2.5 Cytochemistry for SA-β-Galactosidase

To monitor senescence *in situ*, cells were stained for SA-β-galactosidase activity as described (Greussing et al., 2013). While melanocytes were incubated in staining solution overnight before imaging, fibroblasts were stained for complete 24 h. Blue staining, indicative of SA-β-Gal activity, was documented by phase-contrast microscopy (Nikon

Eclipse TE300 microscope connected to a Nikon Digital Sight DS-U2 camera – Nikon, The Netherlands). The percentage of positive cells was calculated by dividing the number of positive blue cells by the total number of cells in a given plate. At least 100 cells per group were counted for each experiment. Three independent experiments were performed.

2.6 Protein isolation and western blotting

Protein lysates were prepared as described (Lener et al., 2009). Appropriate amounts of protein were separated by SDS-PAGE electrophoresis and transferred to PVDF membranes as described (Greussing et al., 2013). Proteins of interest were detected by incubating the membranes with appropriate antibodies. Following primary antibodies were used: monoclonal mouse anti-p53 (#SC-126 Santa Cruz Biotechnology, USA), polyclonal rabbit anti-Lamin B1 (#ab16048 Abcam, United Kingdom), monoclonal rabbit anti-p21 waf1/cip1 (#2947S Cell signaling technology, USA), polyclonal rabbit anti-pp53 (Serin15) (#9284S Cell signaling technology, USA), and monoclonal mouse anti-GAPDH - glyceraldehyde 3-phosphate dehydrogenase (GAPDH) (#SC-25778 Santa Cruz Biotechnology, USA). Appropriate polyclonal HRP-conjugated secondary antibodies were used (Dako Cytomation, Denmark). Detection was performed in a ChemiDoc Imaging system (Bio-Rad Laboratories, USA) using a chemiluminescence substrate kit (Merck Millipore, Germany). As positive controls protein lysates obtained from HDFs at passage 35 and Cisplatin-treated HDFs (33 μM) were used. Results were normalized to the loading control. Analysis of densitometry was performed in ImageJ software and the values were normalized to the loading control (GAPDH).

2.7 Monitoring proteasome activity by FACS

Analysis of proteasome activity was carried out by measuring the fluorescence of melanocytes expressing the GFP-degron fusion protein by flow cytometry as described (Greussing et al., 2012). For every measurement, a positive control was produced by incubating the infected cells with 100 μM N-acetyl-L-leucyl-L-leucyl-leucyl-L-norleucinal (LLnL) for 3 h. Untransfected cells were used as negative control to determine the correct gating. All measurements were repeated at least three times.

2.8 Detection of specific proteins by Immunofluorescence

Cells were seeded in 6-well plates containing coverslips previously covered in poly-D-lysine (Gibco, Germany). On the day of collection, cells were fixed in 4% paraformaldehyde (PFA), permeabilized (0.3 % Triton-X, 0.1 % sodium citrate in PBS) and incubated with appropriated primary antibodies for 1 h at RT. After washing, the cells were incubated with secondary antibodies, counterstained with DAPI and mounted in fluorescence mounting medium (Dako Cytomation, Denmark).The following primary antibodies were used: monoclonal rabbit anti-Melan-A (#51061 Abcam, United Kingdom), monoclonal mouse anti-Vimentin (#sc-6260 Santa Cruz Biotechnology, USA) and polyclonal rabbit anti-APG7/ATG7 (#PK-AB718-3617 Promocell, Germany). Appropriated Alexa-Fluor conjugated secondary antibodies (Life technologies, USA.) were used. Images were obtained by confocal scanning system Cell Voyager CV1000 (Visitron Systems, Germany). Number of autophagy-related protein 7 (Atg7) puncta per cell was counted in ImageJ software and for each group at least 50 cells were counted from three independent experiments. The

percentage of multinucleated cells was calculated by counting the number of cells with more than one nucleus and dividing by the total number of cells of a certain field. For each group at least 30 cells were counted from three independent experiments.

2.9 Fontana-Masson staining

Cells grown on coverslips were fixed in 4% PFA for 15 min. The incubation of coverslips with ammoniacal silver solution was done for 30 min at 59 °C. Coverslips were washed and incubated for 30 s in 0.2 % gold chloride solution and then in 5% sodium thiosulfate solution for 90 s. For nuclear counterstaining nuclear fast red solution was used. Coverslips were mounted in Entellan (Merck Milipore, Germany). Slides were analyzed in Leica DMLS (Leica Mikroskopie & Systeme GmbH, Germany). Number of melanosomes per cell was counted in ImageJ software. At least 30 cells were counted from three independent experiments.

2.10 Melanin content

Melanocytes were harvested and 1×10^5 cells were used for the measurement. The cells were trypsinized, resuspended in modified RIPA buffer (50 mM Tris-HCl, 150 mM sodium chloride, 1 % NP-40, 0.25 % sodium deoxycholate, 1 mM EDTA, 100 nM sodium orthovanadate, 1 mM sodium fluoride, 10 mM β-glycerophosphate) and sonicated in this same buffer. After sonification, cells were centrifuged at 20,000 *g* for 15 min at 4 °C. The supernatant was collected in a new tube and was incubated with 1 N NaOH/10 % DMSO for 90 min at 80 °C. The absorbance was measured at 492 nm. The determination of melanin content was done by using a standard curve generated from synthetic melanin. All measurements were done at least in three independent triplicates.

2.11 Statistics

Results are displayed as mean values of independent experiments ± standard deviation (SD). Differences were compared using Student's *t* test. In all graphics *p < 0.05; **p < 0.01; ***p < 0.001 and n.s. no statistical significance.

3 Results

3.1 UVB induces changes in proliferation, morphology and ploidy of human epidermal melanocytes

Previous work of our group has demonstrated that mild and repeated doses of UVB lead to stress-induced premature senescence of human dermal fibroblasts (Cavinato et al., 2016; Greussing et al., 2013). Using the same experimental approach, in which cells are subjected to UVB-irradiation twice a day for a period of four consecutive days, we investigated the direct effect of UVB on melanocytes (Fig. 1 A). Initially, to ensure that the melanocyte cultures would not be contaminated by fibroblasts, characterization of melanocytes derived from newborn foreskin was performed by immunofluorescence to detect the presence of the melanocyte marker Melan-A (Sup. Fig. 1). Then, to establish the proper conditions through which UVB induces senescence, melanocytes were submitted to different dosages of UVB and monitored for cell proliferation (Sup. Fig. 2). Control non-irradiated cells performed around 7 population doublings (cPDLs) during the 15 days of experiment. Melanocytes

irradiated with 0.075 and 0.1 J/cm^2 UVB displayed slight growth arrest. Treatment of cells with 0.125 J/cm^2 UVB induced stronger growth arrest, while doses equal to or greater than 0.150 J/cm^2 UVB led to negative cPDL numbers, indicating cell death (Fig. 1 B, S2). Based on these results, the dosage of 0.125 J/cm^2 was defined as standard condition, which was used to perform all the other UVB irradiations of melanocytes described in this work.

Cellular senescence is characterized by cell-cycle arrest and alterations in cell shape and metabolism (Greussing et al., 2013). In this way, cell morphology and number of nuclei per cell of UVB-irradiated and control melanocytes were monitored in order to further characterize the changes caused by UVB (Fig. 1). Analysis of cell surface area revealed that irradiated cells showed a significant increase in size compared to non-irradiated cells (Fig. 1C–D). The observed increase in size coincided with the growth arrest caused by the irradiation (Fig. 1 B). In addition, accumulation of cytoplasmic brown granules, indicative of increased melanin synthesis, was observed in some UVB-irradiated melanocytes (Fig. 1 B, arrows).

In certain cell types, senescence is associated with polyploidy and multinucleation due to cell cycle arrest (Akakura et al., 2010). With regard to melanocytes specifically, the appearance of multinucleated cells is related to both senescence and nevi formation (Leikam et al., 2015). By counting the number of multinucleated cells in UVB and control melanocytes we found that UVB treatment increased percentage of cells with two or more nuclei already on D4 (Fig. 1E). On D9, more than 30 % of UVB irradiated melanocytes presented more than one nucleus and on D15 this percentage was slightly decreased but still around five times higher than observed in control cells (Fig. 1E).

Cytochemistry for the activity of SA-β-Gal and analysis of the regulation of senescence-associated proteins were used to confirm senescence induction by UVB irradiation of melanocytes (Fig. 2). UVB induced the accumulation of SA-β-Gal positive cells (Fig. 2A–B) and a strong but transient phosphorylation of p53 on serine 15 (pp53), most notable at D4, i.e. after application of the last stress, indicative of p53 activation (Fig. 2C–E). In addition, the overall levels of p53 protein were also increased and remained higher than the ones from control cells throughout the experiment. Activation of p53 also resulted in the upregulation of its downstream effector p21^{waf1} (Fig. 2C–E). Expression of the nuclear lamina protein Lamin B1 was initially slightly increased in UVB-irradiated cells. However, on D9, coinciding with the increased activity of SA-β-Gal and expression of other senescence markers, levels of Lamin B1 were significantly lower in irradiated melanocytes than in control cells (Fig. 2C–E). Altogether these results demonstrate that mild and repeated doses of UVB induce senescence of human melanocytes.

3.2 UVB irradiation impairs proteasome activity and increases autophagy in melanocytes

Next, we wanted to investigate if mechanisms of protein quality control would be affected during the process of UVB-induced senescence of melanocytes. To monitor proteasome activity, we generated a reporter cell line consisting of melanocytes expressing a GFP-degron protein. Under physiological conditions, GFP-degron expressing cells show low GFP fluorescence because the destabilized protein is degraded by proteasomes. In contrast, when proteasome activity is blocked, GFP-degron protein cannot be efficiently degraded and

accumulates in the cytoplasm leading to increased green fluorescence (Greussing et al., 2012) (Fig. 3 A). GFP-degron expressing melanocytes were submitted to UVB as described, and proteasome activity was monitored by FACS analysis. Non-transfected cells were used as negative control. As positive controls GFP-degron melanocytes were treated with the protea-some inhibitor N-acetyl-L-leucyl-L-leucyl-leucyl-L-norleucinal (LLnL). UVB treatment led to increased cytoplasmic green fluorescence in comparison to control nonirradiated cells throughout the whole experimental procedure, suggesting significantly impaired proteasome activity (Fig. 3 B).

To address a potential role of autophagy in UVB-induced senescence of melanocytes, cells were further processed for immunofluorescence to label Atg7. The Atg7 protein is involved in the conversion of the microtubule-associated protein light chain 3 (LC3-I) into its lipidated form, LC3-II and is, therefore, essential for the assembly of the autop-hagosomes (Zhang et al., 2015). UVB-irradiated melanocytes presented more Atg7 positive dots in comparison to control non-irradiated cells throughout the whole experiment (Fig. 3C–D). The peak of autophagy was observed on D9 when the mean number of Atg7 positive punctae per cell was four times higher in irradiated melanocytes in comparison with control cells. Taken together these results suggest that the process of UVB-induced senescence of melanocytes involves impairment of proteasome activity and exacerbated autophagic activity.

3.3 UVB irradiation induces the accumulation of melanosomes in melanocytes

During the period of irradiations, we could observe an increased accumulation of brown structures in the cytoplasm of UVB-treated melanocytes (Fig. 1 C, inset and black arrows). This made us hypothesize that the applied UVB dosage could be sufficient to initiate the process of melanogenesis in our cells. To investigate this possibility, we evaluated intracellular melanin content of UVB irradiated and control melanocytes by absorption spectroscopy (Fig. 4 A) and Fontana-Masson (FM) staining (Fig. 4B–C) on the last day of UVB treatment (D4). In comparison to control non-irradiated cells, UVB induced a significant increase in melanin content per cell (Fig. 4 A). Furthermore, irradiation led to a switch in the distribution of cytoplasmic melanosomes, as can be seen from the results obtained by Fontana-Masson staining (Fig. 4B–C). Half of the population of control melanocytes presented maximum 10 melanosomes per cell and less than 4% of this population presented more than 300 melanosomes in their cytoplasm. In contrast, in the group of irradiated cells, only 10 % of the population had zero to 10 melanosomes per cell while the population of cells with more than 300 melanosomes increased to more than 20 %. Collectively these results indicate that accumulation of cytoplasmic melanosomes occurs during the process of UVB-induced senescence of melanocytes.

3.4 Factors secreted by senescent fibroblasts modulate melanocytes' ploidy and melanogenesis in a co-culture system

Recent publications have reported a direct relationship between skin pigmentation and SASP components secreted by dermal fibroblasts (Yoon et al., 2018). Thus, we decided to investigate the potential role of irradiated fibroblasts in the modulation of melanocytes in relation to pigmentation and its underlying mechanisms. For this purpose, human dermal

fibroblasts (HDFs) were irradiated twice a day during 4 consecutive days with 0.05 J/cm^2 UVB and allowed to recover for further 3 days (UVB D7). Senescent status of irradiated and control HDFs was monitored by SA-β-Gal (Sup. Fig. 3). Co-cultures of fibroblasts and melanocytes were established by seeding UVB-irradiated senescent fibroblasts with non-irradiated melanocytes (UVB) or non-irradiated fibroblasts with non-irradiated melanocytes (Ctrl) (Fig. 5 A). After 3 days of co-culture, melanocytes were collected, counted (Suppl. Fig. 4) as well as analyzed for cell surface area (Fig. 5B), number of nuclei per cell (Fig. 5 C), melanin content (Fig. 5D) and number of melanosomes per cell (Fig. 5E–F).

Co-cultivation of melanocytes with UVB-irradiated fibroblasts did not affect melanocyte proliferation (Sup. Fig. 4) and did not change melanocytes' cell surface area (Fig. 5B) However, we observed an increased percentage of melanocytes with two or more nuclei when these cells were cultivated together with UVB-treated HDFs in comparison to the ones cultivated with control non-irradiated HDFs (Fig. 5C). To evaluate the potential effect of HDFs on melanocytes pigmentation we measured intracellular melanin content by absorption spectroscopy (Fig. 5D) and FM staining (Fig. 5E–F). Increased melanin content was observed in melanocytes co-cultivated in the presence of senescent HDFs (Fig. 5 D). Moreover, co-culture with UVB-irradiated HDFs led to a switch in the distribution of cytoplasmic melanosomes in melanocytes, as can be seen from the results obtained by Fontana-Masson staining (Fig. 5E–F). For instance, around 40 % of the population of melanocytes cultivated with control non-irradiated HDFs presented maximum 10 melanosomes per cell while no cell presented more than 300 melanosomes in their cytoplasm. In contrast, when melanocytes were cultivated with irradiated fibroblasts, only 20 % of the population presented0 to 10 melanosomes per cell while the population of cells with more than 300 melanosomes increased to almost 40 % of the total (Fig. 5E–F). Taken together, these results suggest that factors secreted by senescent fibroblasts are able to increase synthesis and accumulation of melanosomes in melanocytes maintained in co-culture.

4 Discussion

Cellular senescence and photoaging have been in the focus of many recent publications, and, in fact, the appearance and accumulation of senescent cells in the skin is a mechanism recognized as part of the aging process of this tissue (Dimri et al., 1995; Ressler et al., 2006; Victorelli et al., 2019). The appearance of senescent melanocytes in the skin is recognized as a tumor suppression mechanism (Tominaga, 2015). However, in-depth knowledge about mechanisms underlying UVB damage to melanocytes and its participation in the processes of skin aging and pigmentation are missing. The aim of this study was to establish a model of UVB-induced senescence of melanocytes in which we could investigate senescence-related pathways already observed in other cell types, such as skin fibroblasts. In addition, we explored the interplay between fibroblasts and melanocytes in order to investigate the potential effect of factors secreted by senescent fibroblasts on melanocytes' biology.

Previous work from our group has shown that mild and repeated doses of UVB induces senescence in early passage human dermal fibroblasts (Cavinato et al., 2016; Greussing et al., 2013). Using this same model, here we demonstrate that UVB-induced senescence of

melano-cytes recapitulates several mechanisms observed in fibroblasts such as cell cycle arrest characterized by activation and stabilization of the p53-p21 pathway and disappearance of the nuclear protein Lamin B1, increased activity of SA-β-Gal, impairment of the ubiquitin-proteasome system and activation of autophagy. In addition, UVB irradiation increased the frequency of multinucleated melanocytes, an event already reported to be related to senescence of these cells and to the occurrence of pigmentation disorders by other investigators (Boyd et al., 2015; Leikam et al., 2015).

Protein homeostasis, described as the balance between synthesis, modification, transport and degradation of proteins in a cell, is an important process modified by cellular aging. During aging, these processes are mostly impaired or decreased leading to accumulation of misfolded proteins (Morimoto and Cuervo, 2014). The two major protein quality control mechanisms active in UV-irradiated skin cells are autophagy and the ubiquitin-proteasome pathway (Wedel et al., 2018). In fibroblasts, UVB irradiation leads to proteasome inactivation and this is compensated by induction of excessive autophagy. In this context, autophagy is essential for the establishment of the senescent phenotype (Cavinato et al., 2016). In addition, in melanocytes, autophagy also plays a specific role in the synthesis, degradation and transport of melanosomes (Ho and Ganesan, 2011; Ramkumar et al., 2017; Yun et al., 2016). Accordingly, autophagy defects in melanocytes can cause skin pigmentary disorders (Wang et al., 2019a). However, the relationship between melanocytes protein quality control, senescence and pigmentation is still poorly explored. Using a GFP-reporter to study proteasome activity and immunofluorescence staining to label the autophagy-related protein Atg7, we have demonstrated that UVB irradiation impairs the proteasomal system and increases autophagic activity in melanocytes. These events coincided with the increase in pigmentation and the appearance of senescence markers such as p53 stabilization and increased synthesis of SA-β-Gal, reinforcing the hypothesis that proteostasis, senescence and pigmentation are interconnected mechanisms in melanocytes.

Skin tanning is an adaptive photoprotective mechanism modulated by exposition to sunlight. It is reported that pigment darkening occurs within minutes after skin is exposed to UV rays and perseveres for a few days. This process is caused by oxidation and polymerization of existing melanin, by the redistribution of existing melanosomes and is induced mainly by UVA. UVB elicits a different photobiological effect, known as delayed tanning, as it is initiated several days after sun exposure and involves true neomelanogenesis through the activation of the melanin synthesis pathway (Kohli et al., 2019; Yamaguchi et al., 2007). Conventional melanin quantification methods are based on absorption spectroscopy, which measures the melanin content from lysed cells but disregards accumulation of melanosomes and consequently, neomelanogenesis. Fontana-Masson staining, on the other hand, is a standard method used to detect argentaffin granules in paraffin sections but is poorly explored for the detection of melanosomes in monolayers of melanocytes. In our model of UVB-induced senescence of melanocytes we have demonstrated that UVB induces significant increase in intracellular melanin, as measured by a colorimetric assay. In addition, we have adapted the current FM protocol for the study of cells grown oncoverslips. By doing so, we showed that the increased melanin content observed after UVB irradiation is related to the accumulation of melanosomes. Hence, we could confirm that FM staining can be successfully applied to demonstrate accumulation and distribution of melanosomes in

Europe PMC Funders Author Manuscripts

response to different conditions. Furthermore, we have confirmed the hypothesis that true neomelanogenesis is elicited in response to mild and repeated doses of UVB.

Skin is a social organ and changes in its appearance, such as pigmentation disorders, can cause significant psychosocial distress and affect people's behavior and quality of life (Cavinato, 2020). Nevertheless, the mechanisms that lead to changes in skin pigmentation during aging have not yet been fully elucidated. Recent publications have reported a direct relationship between skin pigmentation disorders such as melasma, vitiligo and senile lentigos with SASP components secreted by dermal fibroblasts (Espósito et al., 2018; Rani et al., 2017; Yoon et al., 2018). Using a co-culture system consisting of fibroblasts and melanocytes, we investigated the potential role of senescent fibroblasts in the paracrine modulation of some factors related to the biology of melanocytes, which were shown to be altered during melanocytes UVB-induced senescence. In this system, melanocytes co-cultivated with senescent HDFs displayed significant increase in melanin content and higher number of melanosomes per cell, confirming the interplay of melanocytes and fibroblasts in the process of UVB-induced skin pigmentation and reinforcing the fact that factors secreted by senescent HDFs are able to modulate melanogenesis.

In contrast to direct UVB exposure, co-culture with senescent HDFs was not sufficient to affect melanocyte proliferation and cell morphology. However, we observed increased frequency of multinucleated melanocytes when these cells were cultivated with UVB-irradiated fibroblasts. Multinucleated senescent melanocytes are frequently found in human nevi, a common human pigmented lesion (Joselow et al., 2017). However, the dynamics by which senescence signals appear in these cells is unclear. The increased number of multinucleated mela-nocytes observed in our co-culture systems suggested that factors secreted by senescent fibroblasts were able to modulate, at least to some extent, cell cycle regulation in melanocytes. Thus, it is possible that the decrease in cell proliferation and the morphological changes are events that occur after the increase in ploidy during UVB-induced melanocyte senescence. More experiments, where co-culture systems are maintained for longer are necessary to clarify this hypothesis.

In conclusion, here we have demonstrated that mild and repeated doses of UVB induce melanocytes 'senescence in a process that involve impairment of the proteasome system, increased autophagic activity and neomelanogenesis. In addition, using a co-culture system, we could confirm that SASP components secreted by senescent fibroblasts are able to modulate melanogenesis and increase ploidy of melanocytes. Together these two models can be applied to further investigate different aspects of melanocyte biology, skin pigmentation and photoaging.

Supplementary Material

Refer to Web version on PubMed Central for supplementary material.

Acknowledgements

We thank Annabella Pittl for her invaluable help and dedication.

Funding

This work was supported by an award from FWF (P-315820). Maria Cavinato received additional funding by Tiroler Wissenschaftsfonds (ZAP746010) and the same for Sophia Wedel received funding by Aktion D. Swarovski KG 2018, (Projekt Nr. 281886, P7460-030-011).

Abbreviations

Atg7	Autophagy-related protein 7
cPDLs	cumulative population doublings
DAPI	4′6-diamidino-2-phenylindole
D1	Day one
D3	Day three
D4	Day four
D7	Day seven
D9	Day nine
D15	Day fifteen
DMEM	Dulbecco´s modified eagle´s medium
DMSO	Dimethylsulfoxide
EDTA	Ethylenediaminetetraacetic acid
FACS	Fluorescence-activated cell sorting
FCS	Fetal calf serum
FM	Fontana-Masson
GAPDH	Glyceraldehyde 3-phosphate dehydrogenase
GFP-degron	degron-destabilized green fluorescent protein
HEK293-T	Human embryonic kidney 293 cells containing the SV40 T-antigen
HDFs	Human dermal fibroblasts
HSEM	Human skin epidermal melanocytes
LC3	Microtubule-associated protein light chain 3
LLnL	N-acetyl-L-leucyl-L-leucyl-leucyl-L-norleucinal
MMPs	Matrix metalloproteases
NaOH	Sodium hydroxide

PBS	Phosphate buffered saline
PFA	Paraformaldehyde
pp53	Phosphorylation of p53 on serine 15
RIPA	Radioimmunoprecipitation assay buffer
ROS	Reactive oxygen species
RT	Room temperature
SASP	Senescence-associated secretory phenotype
SA-β-Gal	Senescence-associated β-Galactosidase
SD	Standard deviation
U2OS	Human osteosarcoma cell line
UV	Ultraviolet

References

Abd El-Aal, NH, Abd El-Wadood, FA, Moftah, NH, El-Hakeem, MS, El-Shaal, AY, Hassan, NB. Indian J Dermatol. Wolters Kluwer – Medknow Publications; 2012. Morphometry and epidermal fas expression of unexposed aged versus young skin; 181–186.

Akakura S, Nochajski P, Gao L, Sotomayor P, Matsui SI, Gelman IH. Rb-dependent cellular senescence, multinucleation and susceptibility to oncogenic transformation through PKC scaffolding by SSeCKS/AKAP12. Cell Cycle. 2010; 9:4656–4665. DOI: 10.4161/cc.9.23.13974 [PubMed: 21099353]

Baker DJ, Childs BG, Durik M, Wijers ME, Sieben CJ, Zhong JA, Saltness R, Jeganathan KB, Verzosa GC, Pezeshki A, Khazaie K, et al. Naturally occurring p16Ink4a-positive cells shorten healthy lifespan. Nature. 2016; 530:184–189. DOI: 10.1038/nature16932 [PubMed: 26840489]

Barysch MJ, Braun RP, Kolm I, Ahlgrimm-Siesz V, Hofmann-Wellenhof R, Duval C, Warrick E, Bernerd F, Nouveau S, Dummer R. Keratinocytic Malfunction as a trigger for the development of solar lentigines. Dermatopathology. 2019; 6:1–11. DOI: 10.1159/000495404 [PubMed: 30800656]

Bellei B, Picardo M. Premature cell senescence in human skin: dual face in chronic acquired pigmentary disorders. Ageing Res Rev. 2020; 57doi: 10.1016/j.arr.2019.100981

Boyd AS, Chen SC, Shyr Y. Intradermal nevi with atypical nuclei in the elderly: the senescent nevus. J Am Acad Dermatol. 2015; 73:500–506. DOI: 10.1016/j.jaad.2015.06.013 [PubMed: 26188628]

Cavinato, M. Cosmetics and cosmeceuticals. In: Ratan, SI, editor. Reference Module in Biomedical Sciences. Elsevier; 2020. 446–461.

Cavinato M, Jansen-Dürr P. Molecular mechanisms of UVB-induced senescence of dermal fibroblasts and its relevance for photoaging of the human skin. Exp Gerontol. 2017; 94:78–82. DOI: 10.1016/j.exger.2017.01.009 [PubMed: 28093316]

Cavinato M, Koziel R, Romani N, Weinmüllner R, Jenewein B, Hermann M, Dubrac S, Ratzinger G, Grillari J, Schmuth M, Jansen-Dürr P. UVB-induced senescence of human dermal fibroblasts involves impairment of proteasome and enhanced autophagic activity. Journals Gerontol Ser A Biol Sci Med Sci. 2016; 72doi: 10.1093/gerona/glw150.glw150

Cavinato M, Waltenberger B, Baraldo G, Grade CVC, Stuppner H, Jansen-Dürr P. Plant extracts and natural compounds used against UVB-induced photoaging. Biogerontology. 2017; 18:499–516. DOI: 10.1007/s10522-017-9715-7 [PubMed: 28702744]

Choi W, Yin L, Smuda C, Batzer J, Hearing VJ, Kolbe L. Molecular and histological characterization of age spots. Exp Dermatol. 2017; 26:242–248. DOI: 10.1111/exd.13203 [PubMed: 27621222]

Europe PMC Funders Author Manuscripts

Dimri GP, Lee X, Basile G, Acosta M, Scott G, Roskelley C, Medrano EE, Linskens M, Rubelj I, Pereira-Smith O. A biomarker that identifies senescent human cells in culture and in aging skin in vivo. Proc Natl Acad Sci U S A. 1995; 92:9363–9367. DOI: 10.1073/pnas.92.20.9363 [PubMed: 7568133]

Eckhart L, Tschachler E, Gruber F. Autophagic control of skin aging. Front Cell Dev Biol. 2019; 7doi: 10.3389/fcell.2019.00143

Espósito ACC, Brianezi G, de Souza NP, Miot LDB, Marques MEA, Miot HA. Exploring pathways for sustained melanogenesis in facial melasma: an im-munofluorescence study. Int J Cosmet Sci. 2018; 40:420–424. DOI: 10.1111/ics.12468 [PubMed: 29846953]

Greussing R, Unterluggauer H, Koziel R, Maier AB, Jansen-Dürr P. Monitoring of Ubiquitin-proteasome Activity in Living Cells Using a Degron (dgn)-destabilized Green Fluorescent Protein (GFP)-based Reporter Protein. J Vis Exp. 2012; doi: 10.3791/3327

Greussing R, Hackl M, Charoentong P, Pauck A, Monteforte R, Cavinato M, Hofer E, Scheideler M, Neuhaus M, Micutkova L, Mueck C, et al. Identification of microRNA-mRNA functional interactions in UVB-induced senescence of human diploid fibroblasts. BMC Genomics. 2013; 14:224.doi: 10.1186/1471-2164-14-224 [PubMed: 23557329]

Haddad MM, Xu W, Medrano EE. Aging in epidermal melanocytes: cell cycle genes and melanins. J Investig Dermatol Symp Proc. 1998; 3:36–40. DOI: 10.1038/jidsymp.1998.9

Ho H, Ganesan AK. The pleiotropic roles of autophagy regulators in melanogenesis. Pigment Cell Melanoma Res. 2011; 24:595–604. DOI: 10.1111/j.1755-148X.2011.00889.x [PubMed: 21777401]

Hutter E, Renner K, Pfister G, Stöckl P, Jansen-Dürr P, Gnaiger E. Senescence-associated changes in respiration and oxidative phosphorylation in primary human fibroblasts. Biochem J. 2004; 380:919–928. DOI: 10.1042/BJ20040095 [PubMed: 15018610]

Joselow A, Lynn D, Terzian T, Box NF. Senescence-like phenotypes in human nevi. Methods Mol Biol. 2017; :175–184. DOI: 10.1007/978-1-4939-6670-7_17

Kohli I, Sakamaki T, Dong Tian W, Moyal D, Hamzavi IH, Kollias N. The dynamics of pigment reactions of human skin to ultraviolet A radiation. Photodermatol Photoimmunol Photomed. 2019; 35:387–392. DOI: 10.1111/phpp.12497 [PubMed: 31206816]

Krutmann J, Bouloc A, Sore G, Bernard BA, Passeron T. The skin aging exposome. J Dermatol Sci. 2017; 85:152–161. DOI: 10.1016/j.jdermsci.2016.09.015 [PubMed: 27720464]

Leikam C, Hufnagel AL, Otto C, Murphy DJ, Mühling B, Kneitz S, Nanda I, Schmid M, Wagner TU, Haferkamp S, Bröcker EB, et al. In vitro evidence for senescent multinucleated melanocytes as a source for tumor-initiating cells. Cell Death Dis. 2015; 6:e1711–e1711. DOI: 10.1038/cddis.2015.71 [PubMed: 25837487]

Lener B, Koziel R, Pircher H, Hütter E, Greussing R, Herndler-Brandstetter D, Hermann M, Unterluggauer H, Jansen-Dürr P. The NADPH oxidase Nox4 restricts the replicative lifespan of human endothelial cells. Biochem J. 2009; 423:363–374. DOI: 10.1042/BJ20090666 [PubMed: 19681754]

López-Otín C, Blasco MA, Partridge L, Serrano M, Kroemer G. The hallmarks of aging. Cell. 2013; 153:1194–1217. DOI: 10.1016/j.cell.2013.05.039 [PubMed: 23746838]

Morimoto RI, Cuervo AM. Proteostasis and the aging proteome in health and disease. J Gerontol Ser A Biol Sci Med Sci. 2014; 69:S33–S38. DOI: 10.1093/gerona/glu049 [PubMed: 24833584]

Prieux R, Eeman M, Rothen-Rutishauser B, Valacchi G. Mimicking cigarette smoke exposure to assess cutaneous toxicity. Toxicol In Vitro. 2020; 62doi: 10.1016/j.tiv.2019.104664

Ramkumar A, Murthy D, Raja DA, Singh A, Krishnan A, Khanna S, Vats A, Thukral L, Sharma P, Sivasubbu S, Rani R, et al. Classical autophagy proteins LC3B and ATG4B facilitate melanosome movement on cytoskeletal tracks. Autophagy. 2017; 13:1331–1347. DOI: 10.1080/15548627.2017.1327509 [PubMed: 28598240]

Rani S, Bhardwaj S, Srivastava N, Sharma VL, Parsad D, Kumar R. Senescence in the lesional fibroblasts of non-segmental vitiligo patients. Arch Dermatol Res. 2017; 309:123–132. DOI: 10.1007/s00403-016-1713-0 [PubMed: 28078437]

Ressler S, Bartkova J, Niederegger H, Bartek J, Scharffetter-Kochanek K, Jansen-Durr P, Wlaschek M. p16 INK4A is a robust in vivo biomarker of cellular aging in human skin. Aging Cell. 2006; 5:379–389. DOI: 10.1111/j.1474-9726.2006.00231.x [PubMed: 16911562]

Tominaga K. The emerging role of senescent cells in tissue homeostasis and pa-thophysiology Pathobiol. Aging Age-related Dis. 2015; 5doi: 10.3402/pba.v5.27743

Toutfaire M, Bauwens E, Debacq-Chainiaux F. The impact of cellular senescence in skin ageing: a notion of mosaic and therapeutic strategies. Biochem Pharmacol. 2017; 142:1–12. DOI: 10.1016/j.bcp.2017.04.011 [PubMed: 28408343]

Victorelli S, Lagnado A, Halim J, Moore W, Talbot D, Barrett K, Chapman J, Birch J, Ogrodnik M, Meves A, Pawlikowski JS, et al. Senescent human melanocytes drive skin ageing via paracrine telomere dysfunction. EMBO J. 2019; 38:1–18. DOI: 10.15252/embj.2019101982

Waaijer MEC, Gunn DA, Adams PD, Pawlikowski JS, Griffiths CEM, van Heemst D, Slagboom PE, Westendorp RGJ, Maier AB. P16INK4a positive cells in human skin are indicative of local elastic Fiber morphology, facial wrinkling, and perceived age. J Gerontol Ser A Biol Sci Med Sci. 2016; 71:1022–1028. DOI: 10.1093/gerona/glv114 [PubMed: 26286607]

Waldera Lupa DM, Kalfalah F, Safferling K, Boukamp P, Poschmann G, Volpi E, Götz-Rösch C, Bernerd F, Haag L, Huebenthal U, Fritsche E, et al. Characterization of skin aging-associated secreted proteins (SAASP) produced by dermal fibroblasts isolated from intrinsically aged human skin. J Invest Dermatol. 2015; 135:1954–1968. DOI: 10.1038/jid.2015.120 [PubMed: 25815425]

Wang AS, Dreesen O. Biomarkers of cellular senescence and skin aging. Front Genet. 2018; 9:247.doi: 10.3389/fgene.2018.00247 [PubMed: 30190724]

Wang X, Li S, Liu L, Jian Z, Cui T, Yang Y, Guo S, Yi X, Wang G, Li C, Gao T, et al. Role of the aryl hydrocarbon receptor signaling pathway in promoting mitochondrial biogenesis against oxidative damage in human melanocytes. J Dermatol Sci. 2019a; 96:33–41. DOI: 10.1016/j.jdermsci.2019.09.001 [PubMed: 31543430]

Wang Y, Wen X, Hao D, Zhou M, Li X, He G, Jiang X. Insights into autophagy machinery in cells related to skin diseases and strategies for therapeutic modulation. Biomed Pharmacother. 2019b; 113doi: 10.1016/j.biopha.2019.108775

Wedel S, Manola M, Cavinato M, Trougakos I, Jansen-Dürr P. Targeting protein quality control mechanisms by natural products to promote healthy ageing. Molecules. 2018; 23:1219.doi: 10.3390/molecules23051219

Yamaguchi Y, Brenner M, Hearing VJ. The regulation of skin pigmentation. J Biol Chem. 2007; 282:27557–27561. DOI: 10.1074/jbc.R700026200 [PubMed: 17635904]

Yoon JE, Kim Y, Kwon S, Kim M, Kim YH, Kim J-H, Park TJ, Kang HY. Senescent fibroblasts drive ageing pigmentation: a potential therapeutic target for senile lentigo. Theranostics. 2018; 8:4620–4632. DOI: 10.7150/thno.26975 [PubMed: 30279727]

Yun WJ, Kim E, Park J, Jo SY, Bang SH, Chang E-J, Chang SE. Microtubule-associated protein light chain 3 is involved in melanogenesis via regulation of MITF expression in melanocytes. Sci Rep. 2016; 6doi: 10.1038/srep19914

Zhang C-F, Gruber F, Ni C, Mildner M, Koenig U, Karner S, Barresi C, Rossiter H, Narzt M-S, Nagelreiter IM, Larue L, et al. Suppression of autophagy dysregulates the antioxidant response and causes premature senescence of melanocytes. J Invest Dermatol. 2015; 135:1348–1357. DOI: 10.1038/jid.2014.439 [PubMed: 25290687]

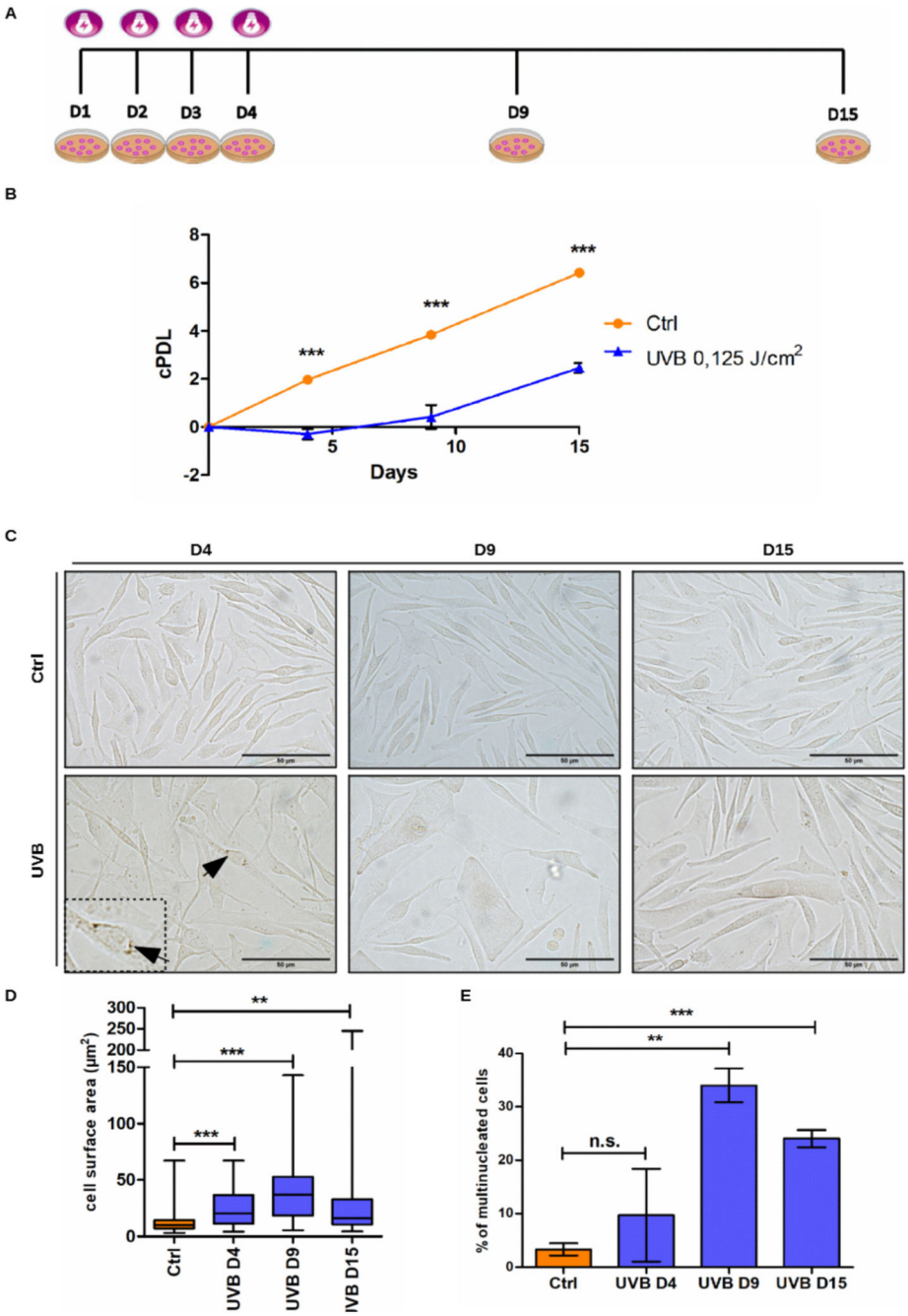

Fig. 1.

UVB affects proliferation, morphology and ploidy of human epidermal melanocytes. **(A)** Graphic representation of the experimental model in which cells are subjected to UVB-irradiation twice a day for a period of four consecutive days and maintained in culture for further 11 days. **(B-E)** Melanocytes were submitted to 0.125 J/cm^2 UVB as described and monitored for cell growth (B) cell morphology (C-D) and percentage of multinucleated cells (E). **(B)** Growth curve of UVB-irradiated and control melanocytes. **(C)** Representative pictures of UVB-irradiated melanocytes and the respective controls obtained on day 4, 9 and

15 of the experiment. Black arrows indicate the accumulation of melanin in UVB treated mel-anocytes. Scale bar 50 μm. **(D)** Analysis of cell surface area. (E) Percentage of multinucleated cells on D4, D9 and D15. Results are presented as mean values ± SD of at least three independent experiments. * < 0.05; **< 0.01; *** < 0.001 and n.s. no statistical significance.

Europe PMC Funders Author Manuscripts

Europe PMC Funders Author Manuscripts

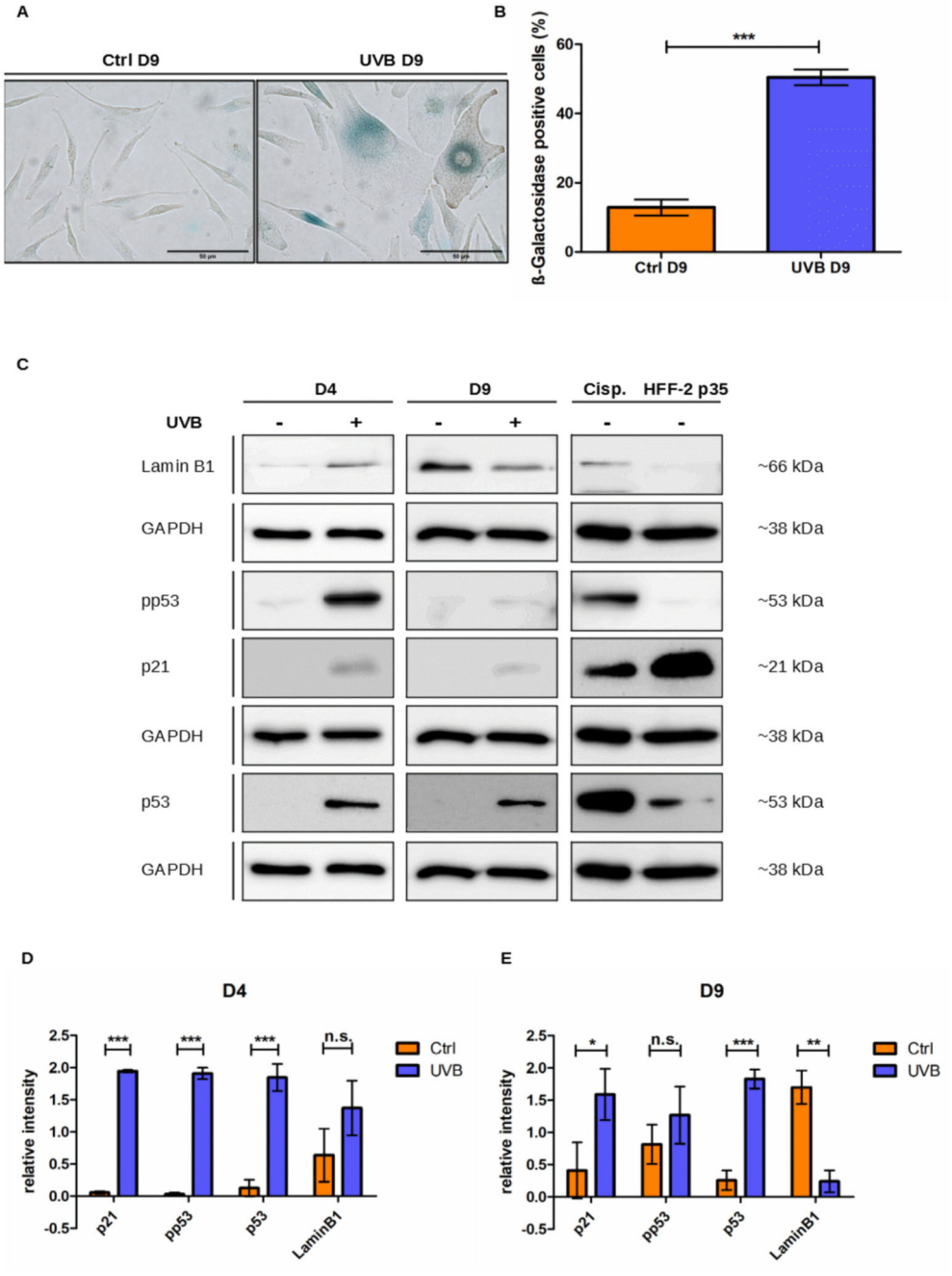

Fig. 2.

UVB induces senescence in human epidermal melanocytes. **(A)** Representative pictures of control and UVB-irradiated mela-nocytes stained for SA-β-Gal on D9 of the experiment. Scale bar 50 μm. **(B)** Percentage of SA-β-Gal positive melanocytes. For each group at least 300 cells were analyzed. **(C)** p21, pp53 (serin 15), p53 and Lamin B1 protein expression of UVB-irradiated and the respective control cells were analyzed by western blot on days 4 and 9 of the experiment. Representative pictures are shown. Lysates from HDFs passage 35 and HDFs treated with 33 μM Cisplatin were used as positive controls. GAPDH was used as a

protein loading control. **(D-E)**– Analysis of relative intensity of the Western blot on days 4 (D) and 9 (E) was performed in ImageJ software. Results are presented as mean values ± SD of at least 3 independent experiments. * < 0.05; ** < 0.01; *** < 0.001 and n.s. no statistical significance.

Europe PMC Funders Author Manuscripts

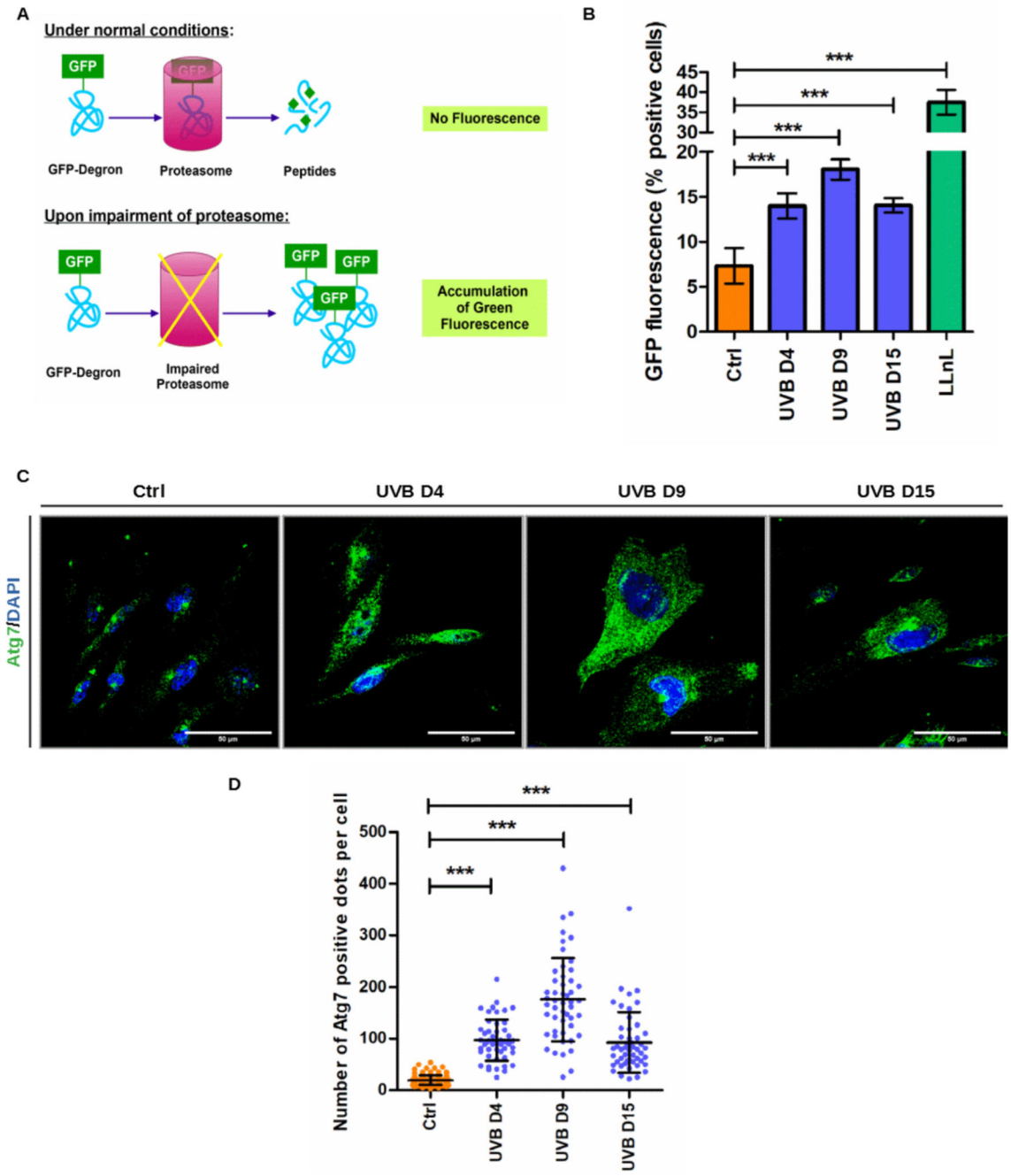

Fig. 3.

UVB impairs proteasome activity and induces autophagy in melanocytes. **(A)** Schematic representation of GFP-degron system to monitor proteasome activity in living cells. **(B)** Melanocytes were irradiated with UVB and green fluorescence resulting from proteasome inactivation was analyzed by flow cytometry. **(C)** UVB-irradiated and control melanocytes processed for immunofluorescence to label Atg7. Representative pictures are shown. Scale bar 50 μm. (D) Number of Atg7 puncta per cell was counted in ImageJ software. Results are presented as mean values ± SD of at least three independent experiments. * < 0.05; ** <

Europe PMC Funders Author Manuscripts

0.01; *** < 0.001 and n.s. no statistical significance (For interpretation of the references to colour in this figure legend, the reader is referred to the web version of this article).

Europe PMC Funders Author Manuscripts

Europe PMC Funders Author Manuscripts

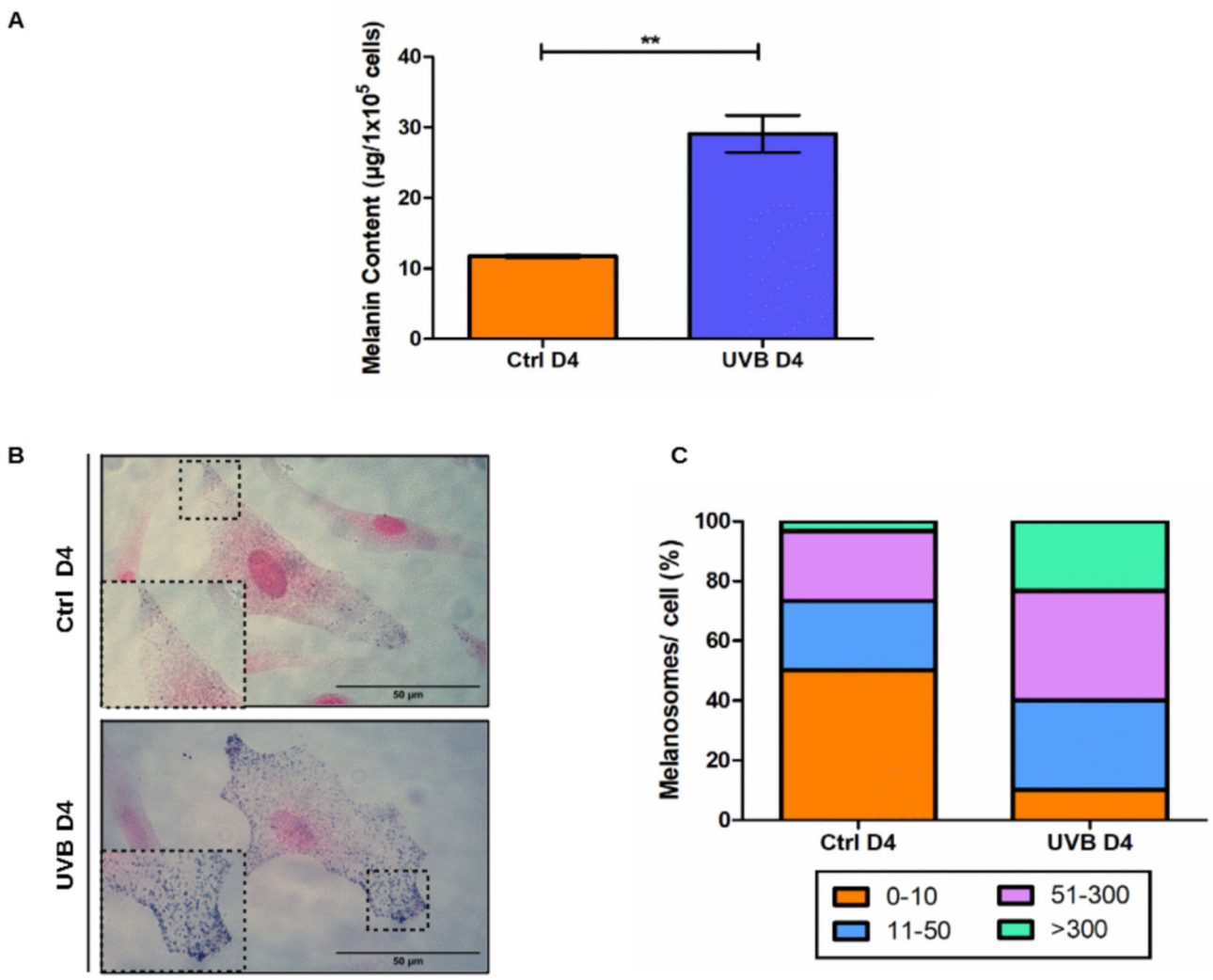

Fig. 4.

UVB leads to accumulation of melano-somes in melanocytes. **(A)** Intracellular melanin content measurement on D4. Bars represent mean values of three independent experiments ± SD. **(B)** Representative picture of the FM staining for Ctrl and UVB-irradiated melanocytes. Inset of dashed regions details distribution of melanosomes in cell cytoplasm. Scale bar 50 µm. **(C)** Quantification of number of melanosomes per cell after FM staining of melanocytes on D4. Stained cells were separated into groups with different amounts of melanosomes per cell. Graphic represents the percentual composition of UVB and control populations in respect to the distribution of melanocytes per cell. Results are presented as mean values ± SD of three independent experiments. * < 0.05; ** < 0.01; *** < 0.001 and n.s. no statistical significance.

Europe PMC Funders Author Manuscripts

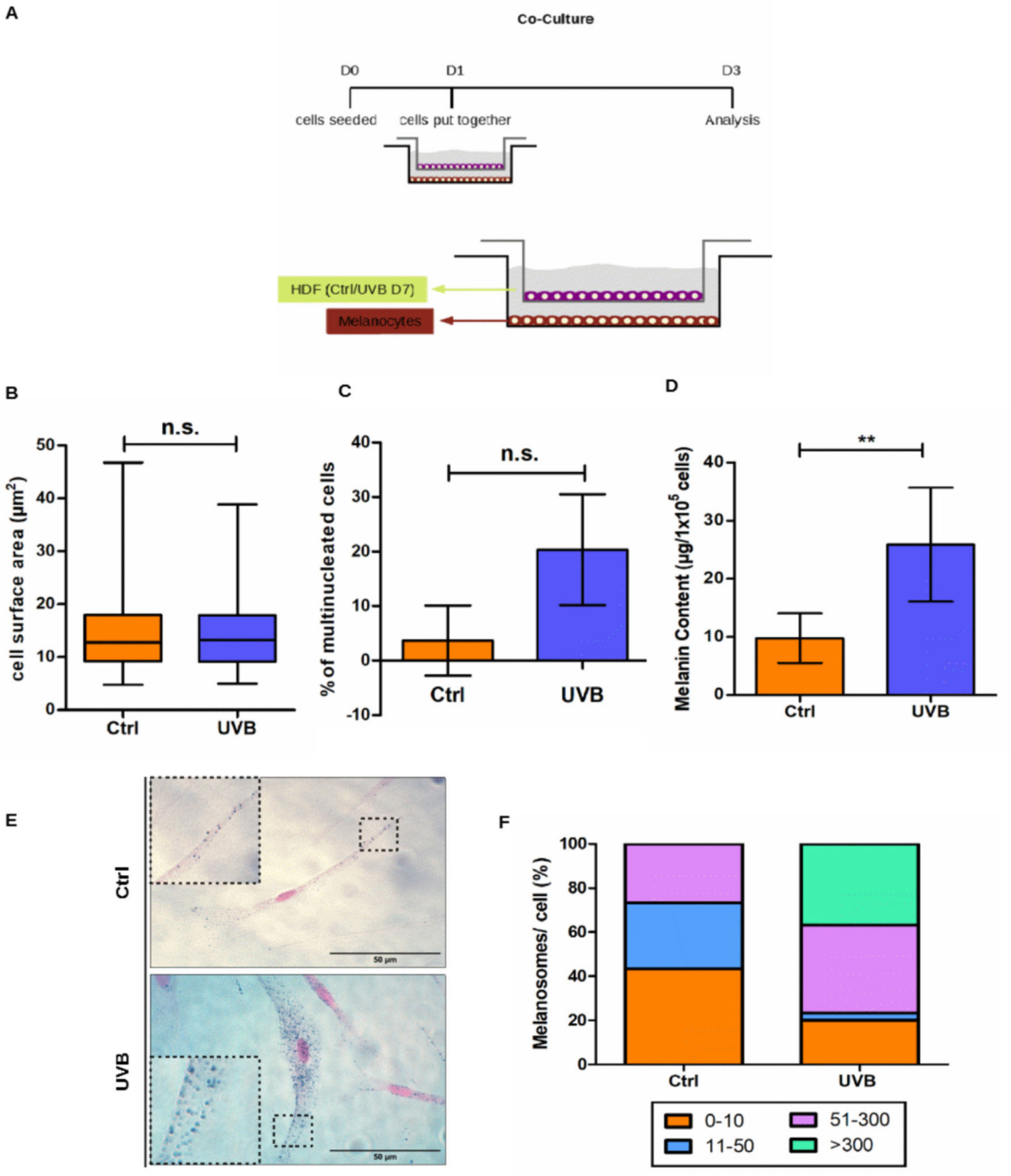

Fig. 5.

Presence of UVB-irradiated HDFs induces multinucleation and modulate melanogenesis of melanocytes in a co-culture system. **(A)** Schematic representation of the experimental setup for co-culture. **(B)** Analysis of cell surface area was performed in ImageJ. At least 30 cells from three independent experiments were analyzed. **(C)** Percentage of multinucleated cells was calculated for melanocytes cultivated in the presence of UVB-irradiated or control HDFs on D3. **(D)** Intracellular melanin content measurement was performed on D3 of co-culture. Bars represent mean values of three independent experiments ± SD. **(E)**

Representative pictures of melanocytes stained by FM. Scale bar 50 μm. Insets display detail of cytoplasmic regions containing melanosomes **(F)** The FM stained melanocytes were separated into groups according to the number of melanosomes per cell. Results are presented as mean values ± SD of three independent replicates. * < 0.05; ** < 0.01; *** < 0.001 and n.s. no statistical significance.

Europe PMC Funders Author Manuscripts